





Coupled Coarray Tensor CPD for DOA Estimation With Coprime L-Shaped Array

Hang Zheng , *Graduate Student Member, IEEE*, Zhiguo Shi , *Senior Member, IEEE*,
Chengwei Zhou , *Member, IEEE*, Martin Haardt , *Fellow, IEEE*, and Jian Chen

Abstract—Conventional canonical polyadic decomposition (CPD) approach for tensor-based sparse array direction-of-arrival (DOA) estimation typically partitions the coarray statistics to generate a full-rank coarray tensor for decomposition. However, such an operation ignores the spatial relevance among the partitioned coarray statistics. In this letter, we propose a coupled coarray tensor CPD-based two-dimensional DOA estimation method for a specially designed coprime L-shaped array. In particular, a shifting coarray concatenation approach is developed to factorize the partitioned fourth-order coarray statistics into multiple coupled coarray tensors. To make full use of the inherent spatial relevance among these coarray tensors, a coupled coarray tensor CPD approach is proposed to jointly decompose them for high-accuracy DOA estimation in a closed-form manner. According to the uniqueness condition analysis on the coupled coarray tensor CPD, an increased number of degrees-of-freedom for the proposed method is guaranteed.

Index Terms—Coarray tensor, coprime L-shaped array, coupled CPD, DOA estimation.

I. INTRODUCTION

Tensor-based direction-of-arrival (DOA) estimation using sparse arrays [1]–[8] has been an important topic since it can preserve the original structure of multi-dimensional received signals beyond the Nyquist sampling rate [9]–[12]. To increase the number of degrees-of-freedom (DOFs), augmented virtual arrays were derived from the second-order statistics of sparse arrays [13]–[17], where canonical polyadic decomposition (CPD) has been the typical approach to process the

corresponding coarray statistics for retrieving angle information [18]–[20]. To solve the rank deficiency problem of the resulting coarray tensor, the ordinary CPD-based methods require the coarray statistics to be partitioned and then averaged to a full-rank coarray tensor [18]–[20], where the ignorance of spatial relevance among these partitioned coarray statistics results in a performance deterioration for DOA estimation. Therefore, how to effectively process the coarray statistics for tensor-based sparse array DOA estimation is still at the initial stage.

To handle the multiple tensors sampled from colocated antenna arrays, the idea of coupled CPD has been proposed to jointly decompose those tensors for transmitted symbol estimation [21]. Since then, the coupled CPD approach has been introduced for harmonic retrieval [22], [23], blind source separation [24], joint channel and symbol estimation [25], image fusion [26], [27], and MEG/EEG signal processing [28], [29]. However, these existing methods assume that the Nyquist sampling theorem holds, which is not the case for signals that are received by sparse arrays. To establish the relationship between the coupled CPD and sparse linear array signal processing, a coupled CPD-based multiple invariance ESPRIT method is reported in [30], which is further extended to generalized sparse array geometries [31]. Nevertheless, since these ESPRIT-like methods directly factorize the first-order signals into multiple coupled tensors instead of deriving virtual arrays, they fail to increase the number of DOFs for DOA estimation. Therefore, it is still challenging to incorporate the coupled CPD to sparse arrays for coarray tensor-based DOA estimation with an increased number of DOFs.

In this letter, we propose a coupled coarray tensor CPD-based two-dimensional DOA estimation method for a designed coprime L-shaped array (CLSA) composed of two separated coprime linear arrays. The cross-correlation-based fourth-order coarray statistics are calculated to avoid the noise power perturbation. Then, different from averaging the partitioned coarray statistics as the conventional approaches did, a shifting coarray concatenation approach is developed to factorize these partitioned coarray statistics into multiple coupled coarray tensors. To exploit the spatial relevance among these coarray tensors, a coupled coarray tensor CPD approach is developed to jointly decompose them for two-dimensional DOA estimation. Moreover, based on the uniqueness condition analysis on the coupled coarray tensor CPD, the proposed method is capable of achieving an increased number of DOFs. Simulation results demonstrate that the proposed coupled coarray tensor CPD-based method presents a superior DOA estimation accuracy than the ordinary CPD-based methods for the CLSA.

Manuscript received April 24, 2021; revised July 7, 2021; accepted July 16, 2021. Date of publication July 26, 2021; date of current version August 12, 2021. This work was supported in part by the National Natural Science Foundation of China under Grants U1909207, 61901413, and 61772467, in part by the Consulting Research Project of the Chinese Academy of Engineering under Grant 2019-XZ-7, in part by the National Key R&D Program of China under Grant 2018YFE0126300, and in part by the 5G Open Laboratory of Hangzhou Future Sci-Tech City. The associate editor coordinating the review of this manuscript and approving it for publication was Dr. Koby Todros. (Corresponding author: Chengwei Zhou.)

Hang Zheng and Chengwei Zhou are with the College of Information Science and Electronic Engineering, Zhejiang University, Hangzhou 310027, China (e-mail: hangzheng@zju.edu.cn; zhouchw@zju.edu.cn).

Zhiguo Shi is with the College of Information Science and Electronic Engineering, Zhejiang University, Hangzhou 310027, China, and also with the Alibaba-Zhejiang University Joint Research Institute of Frontier Technologies, Hangzhou 310027, China (e-mail: shizg@zju.edu.cn).

Martin Haardt is with the Communications Research Laboratory, Ilmenau University of Technology, Ilmenau 98693, Germany (e-mail: martin.haardt@tu-ilmenau.de).

Jian Chen is with the State Key Laboratory of Fluid Power and Mechatronic Systems, School of Mechanical Engineering, Zhejiang University, Hangzhou 310027, China (e-mail: mjchen@zju.edu.cn).

Digital Object Identifier 10.1109/LSP.2021.3099074

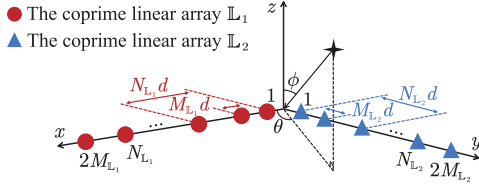


Fig. 1. The geometry of the designed coprime L-shaped array.

II. FOURTH-ORDER TENSOR STATISTICS FOR COPRIME L-SHAPED ARRAY

We design a coprime L-shaped array consisting of two orthogonally placed coprime linear arrays \mathbb{L}_i with $|\mathbb{L}_i| = 2M_{\mathbb{L}_i} + N_{\mathbb{L}_i} - 1$ sensors in the x, y -axes as shown in Fig. 1, $i=1, 2$, where $|\cdot|$ denotes the cardinality of a set. In contrast to the traditional L-shaped array [32], [33], the location of the first sensor in each coprime linear array \mathbb{L}_i starts from 1 instead of 0 in the respective coordinate axis to maintain these two coprime linear arrays separated. Each coprime linear array \mathbb{L}_i can be decomposed into a pair of sparse uniform linear subarrays with $2M_{\mathbb{L}_i}$ and $N_{\mathbb{L}_i}$ sensors, whose inter-element spacings are $N_{\mathbb{L}_i}d$ and $M_{\mathbb{L}_i}d$, respectively. Here, $M_{\mathbb{L}_i}$ and $N_{\mathbb{L}_i}$ are coprime integers with $M_{\mathbb{L}_i} < N_{\mathbb{L}_i}$, and d equals to a half source wavelength. The sensors in \mathbb{L}_1 and \mathbb{L}_2 are respectively located at $\{(x_{\mathbb{L}_1}, 0) | x_{\mathbb{L}_1} = [q_{\mathbb{L}_1}^{(1)}, q_{\mathbb{L}_1}^{(2)}, \dots, q_{\mathbb{L}_1}^{(|\mathbb{L}_1|)}]d\}$ and $\{(0, y_{\mathbb{L}_2}) | y_{\mathbb{L}_2} = [q_{\mathbb{L}_2}^{(1)}, q_{\mathbb{L}_2}^{(2)}, \dots, q_{\mathbb{L}_2}^{(|\mathbb{L}_2|)}]d\}$ with $q_{\mathbb{L}_1}^{(1)} = q_{\mathbb{L}_2}^{(1)} = 1$.

Assume that there are K uncorrelated far-field narrowband sources impinging on the designed CLSA from directions (θ_k, ϕ_k) , where $\theta_k \in [0, \pi]$ and $\phi_k \in [-\pi/2, \pi/2]$ are the azimuth and elevation angles of the k -th source, $k = 1, 2, \dots, K$. The signals received by the coprime linear arrays \mathbb{L}_i with T snapshots can be represented as

$$\mathbf{X}_{\mathbb{L}_i} = \sum_{k=1}^K \mathbf{a}_{\mathbb{L}_i}(k) \circ \mathbf{s}_k + \mathbf{N}_{\mathbb{L}_i} \in \mathbb{C}^{|\mathbb{L}_i| \times T}, \quad (1)$$

where $\mathbf{a}_{\mathbb{L}_i}(k) = [e^{-j\pi q_{\mathbb{L}_i}^{(1)} \mu_i(k)}, e^{-j\pi q_{\mathbb{L}_i}^{(2)} \mu_i(k)}, \dots, e^{-j\pi q_{\mathbb{L}_i}^{(|\mathbb{L}_i|)} \mu_i(k)}]^T$ is the steering vector of \mathbb{L}_i corresponding to the k -th source with directional parameters $\mu_1(k) = \sin \phi_k \cos \theta_k$ and $\mu_2(k) = \sin \phi_k \sin \theta_k$. $\mathbf{s}_k = [s_k(1), s_k(2), \dots, s_k(T)]^T$ is the source waveform vector, and $\mathbf{N}_{\mathbb{L}_i} \sim \mathcal{CN}(\mathbf{0}, \sigma_n^2 \mathbf{I})$ is the additive Gaussian noise. Here, σ_n^2 denotes the noise power, \mathbf{I} denotes the identity matrix, $j = \sqrt{-1}$, \circ denotes the outer product, and $(\cdot)^T$ denotes the transpose operator.

To calculate the second-order statistics of sparse arrays, the conventional auto-correlation of $\mathbf{X}_{\mathbb{L}_i}$ introduces the noise term $\mathbb{E}\{\mathbf{N}_{\mathbb{L}_i} \mathbf{N}_{\mathbb{L}_i}^H\} = \sigma_n^2 \mathbf{I}$ into the covariance matrix of the CLSA, which disturbs the subsequent coarray processing. Here, $\mathbb{E}\{\cdot\}$ denotes the statistical expectation, and $(\cdot)^H$ denotes the conjugate transpose operator. In this regard, we consider to calculate the cross-correlation matrix $\mathbf{R}_{\mathbb{L}_1 \mathbb{L}_2} \in \mathbb{C}^{|\mathbb{L}_1| \times |\mathbb{L}_2|}$ of the two separated coprime linear arrays \mathbb{L}_1 and \mathbb{L}_2 , i.e.,

$$\mathbf{R}_{\mathbb{L}_1 \mathbb{L}_2} = \mathbb{E}\{\mathbf{X}_{\mathbb{L}_1} \mathbf{X}_{\mathbb{L}_2}^H\} = \sum_{k=1}^K \sigma_k^2 \mathbf{a}_{\mathbb{L}_1}(k) \circ \mathbf{a}_{\mathbb{L}_2}^*(k), \quad (2)$$

where $\sigma_k^2 = \mathbb{E}\{s_k(t) s_k^*(t)\}$ is the k -th source power, and $(\cdot)^*$ denotes the conjugate operator. It is clear from (2) that the noise term $\sigma_n^2 \mathbf{I}$ is excluded from the cross-correlation matrix $\mathbf{R}_{\mathbb{L}_1 \mathbb{L}_2}$. However, the steering vectors $\mathbf{a}_{\mathbb{L}_1}(k)$ and $\mathbf{a}_{\mathbb{L}_2}(k)$ in (2) contain different parameters $\mu_1(k)$ and $\mu_2(k)$, which fails to define a

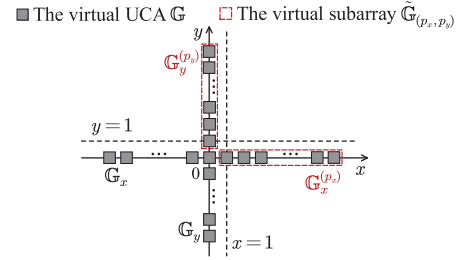


Fig. 2. Illustration of the virtual array segmentation procedure.

difference set that corresponds to an augmented virtual array. Therefore, to increase the number of DOFs for DOA estimation, we propose to use the fourth-order statistics of \mathbb{L}_1 and \mathbb{L}_2 , and a fourth-order tensor $\mathcal{R} = \mathbf{R}_{\mathbb{L}_1 \mathbb{L}_2} \circ \mathbf{R}_{\mathbb{L}_1 \mathbb{L}_2}^* = \mathbb{E}\{(\mathbf{X}_{\mathbb{L}_1} \mathbf{X}_{\mathbb{L}_2}^H) \circ (\mathbf{X}_{\mathbb{L}_1} \mathbf{X}_{\mathbb{L}_2}^H)^*\} \in \mathbb{C}^{|\mathbb{L}_1| \times |\mathbb{L}_2| \times |\mathbb{L}_1| \times |\mathbb{L}_2|}$ is obtained as

$$\mathcal{R} = \sum_{k=1}^K \sigma_k^4 \mathbf{a}_{\mathbb{L}_1}(k) \circ \mathbf{a}_{\mathbb{L}_2}^*(k) \circ \mathbf{a}_{\mathbb{L}_1}^*(k) \circ \mathbf{a}_{\mathbb{L}_2}(k), \quad (3)$$

where the conjugate steering vector pairs $\{\mathbf{a}_{\mathbb{L}_1}(k), \mathbf{a}_{\mathbb{L}_1}^*(k)\}$ and $\{\mathbf{a}_{\mathbb{L}_2}(k), \mathbf{a}_{\mathbb{L}_2}^*(k)\}$ allow a two-dimensional augmented virtual array formulation. In practice, we use the sample fourth-order tensor $\hat{\mathcal{R}} = (1/T \mathbf{X}_{\mathbb{L}_1} \mathbf{X}_{\mathbb{L}_2}^H) \circ (1/T \mathbf{X}_{\mathbb{L}_1} \mathbf{X}_{\mathbb{L}_2}^H)^*$.

III. PROPOSED DOA ESTIMATION METHOD

A. Fourth-Order Tensor Reshaping for Coarray Signals

To derive an augmented virtual array associated with the designed CLSA, we combine the dimensions of the fourth-order tensor \mathcal{R} that represent the angular information along the same coordinate axis. Specifically, defining the dimension sets $\{1, 3\}$ and $\{2, 4\}$, \mathcal{R} is reshaped into the equivalent fourth-order signals of an augmented discontinuous virtual array \mathbb{V} , i.e., $\mathbf{V}_{\mathbb{V}} \triangleq \mathcal{R}_{\{1,3\},\{2,4\}} \in \mathbb{C}^{|\mathbb{L}_1|^2 \times |\mathbb{L}_2|^2}$, as

$$\mathbf{V}_{\mathbb{V}} = \sum_{k=1}^K \sigma_k^4 (\mathbf{a}_{\mathbb{L}_1}^*(k) \otimes \mathbf{a}_{\mathbb{L}_1}(k)) \circ (\mathbf{a}_{\mathbb{L}_2}(k) \otimes \mathbf{a}_{\mathbb{L}_2}^*(k)), \quad (4)$$

where \otimes denotes the Kronecker product. By extracting the contiguous part from \mathbb{V} , a virtual uniform cross array (UCA) $\mathbb{G} = \mathbb{G}_x \cup \mathbb{G}_y$ consisting of two virtual uniform linear arrays (ULAs) $\mathbb{G}_x = \{(x_{\mathbb{G}}, 0) | x_{\mathbb{G}} = [q_{\mathbb{G}_x}^{(1)}, q_{\mathbb{G}_x}^{(2)}, \dots, q_{\mathbb{G}_x}^{(|\mathbb{G}_x|)}]d\}$ and $\mathbb{G}_y = \{(0, y_{\mathbb{G}}) | y_{\mathbb{G}} = [q_{\mathbb{G}_y}^{(1)}, q_{\mathbb{G}_y}^{(2)}, \dots, q_{\mathbb{G}_y}^{(|\mathbb{G}_y|)}]d\}$ as shown in Fig. 2 is obtained, where $q_{\mathbb{G}_x}^{(1)} = -M_{\mathbb{L}_1} N_{\mathbb{L}_1} - M_{\mathbb{L}_1} + 2$, $q_{\mathbb{G}_x}^{(|\mathbb{G}_x|)} = M_{\mathbb{L}_1} N_{\mathbb{L}_1} + M_{\mathbb{L}_1}$, $q_{\mathbb{G}_y}^{(1)} = -M_{\mathbb{L}_2} N_{\mathbb{L}_2} - M_{\mathbb{L}_2} + 2$ and $q_{\mathbb{G}_y}^{(|\mathbb{G}_y|)} = M_{\mathbb{L}_2} N_{\mathbb{L}_2} + M_{\mathbb{L}_2}$. Here, $|\mathbb{G}_x| = 2(M_{\mathbb{L}_1} N_{\mathbb{L}_1} + M_{\mathbb{L}_1}) - 1$ and $|\mathbb{G}_y| = 2(M_{\mathbb{L}_2} N_{\mathbb{L}_2} + M_{\mathbb{L}_2}) - 1$. Accordingly, the fourth-order coarray signals $\bar{\mathbf{V}}_{\mathbb{G}} \in \mathbb{C}^{|\mathbb{G}_x| \times |\mathbb{G}_y|}$ of \mathbb{G} can be obtained by reorganizing the elements of $\mathbf{V}_{\mathbb{V}}$ to map the locations of the corresponding virtual sensors in \mathbb{G} , defined as

$$\bar{\mathbf{V}}_{\mathbb{G}} = \sum_{k=1}^K \sigma_k^4 \mathbf{b}_x(k) \circ \mathbf{b}_y(k), \quad (5)$$

where $\mathbf{b}_x(k) = [e^{-j\pi q_{\mathbb{G}_x}^{(1)} \mu_1(k)}, e^{-j\pi q_{\mathbb{G}_x}^{(2)} \mu_1(k)}, \dots, e^{-j\pi q_{\mathbb{G}_x}^{(|\mathbb{G}_x|)} \mu_1(k)}]^T$ and $\mathbf{b}_y(k) = [e^{-j\pi q_{\mathbb{G}_y}^{(1)} \mu_2(k)}, e^{-j\pi q_{\mathbb{G}_y}^{(2)} \mu_2(k)}, \dots, e^{-j\pi q_{\mathbb{G}_y}^{(|\mathbb{G}_y|)} \mu_2(k)}]^T$ are the steering vectors of \mathbb{G}_x and \mathbb{G}_y , respectively.

Since $\bar{\mathbf{V}}_{\mathbb{G}}$ behaves like the equivalent single-snapshot signals of the virtual UCA \mathbb{G} , its resulting coarray tensor is rank-deficient. To address this problem, the traditional spatial smoothing-based approaches segment \mathbb{G} into several subarrays and average the partitioned coarray statistics to a full-rank coarray tensor for a direct CPD [18]–[20]. However, such an operation suffers from a deteriorated coarray tensor CPD performance due to the ignorance of the spatial relevance among the partitioned coarray statistics. Therefore, it is necessary to develop a more effective coarray tensor processing strategy to make full use of these relevant coarray statistics.

B. Shifting Coarray Concatenation for Coupled Coarray Tensors

To exploit the inherent spatial relevance among the coarray statistics of the designed CLSA, we propose a shifting coarray concatenation approach to factorize these coarray statistics into multiple coupled coarray tensors. Specifically, considering that the virtual ULAs \mathbb{G}_x and \mathbb{G}_y are respectively symmetric to the $x=1$ and the $y=1$ axes as shown in Fig. 2, we select the initial shifting windows $\mathbb{G}_x^{(1)} = \{(x_{\mathbb{G}}^{(1)}, 0) | x_{\mathbb{G}}^{(1)} = [1, 2, \dots, q_{\mathbb{G}_x^{(1)}}]d\}$ and $\mathbb{G}_y^{(1)} = \{(0, y_{\mathbb{G}}^{(1)}) | y_{\mathbb{G}}^{(1)} = [1, 2, \dots, q_{\mathbb{G}_y^{(1)}}]d\}$ from \mathbb{G}_x and \mathbb{G}_y , respectively. Then, by sequentially shifting $\mathbb{G}_x^{(1)}$ along the x -axis by one step, P_x virtual subarrays $\mathbb{G}_x^{(p_x)} = \{(x_{\mathbb{G}}^{(p_x)}, 0) | x_{\mathbb{G}}^{(p_x)} = [2 - p_x, 3 - p_x, \dots, q_{\mathbb{G}_x^{(1)}} + 1 - p_x]d\}$, $p_x = 1, 2, \dots, P_x$, are segmented from \mathbb{G}_x , where $P_x = (|\mathbb{G}_x| + 1)/2$. Similarly, the virtual ULA \mathbb{G}_y can also be segmented into P_y virtual subarrays $\mathbb{G}_y^{(p_y)} = \{(0, y_{\mathbb{G}}^{(p_y)}) | y_{\mathbb{G}}^{(p_y)} = [2 - p_y, 3 - p_y, \dots, q_{\mathbb{G}_y^{(1)}} + 1 - p_y]d\}$, $p_y = 1, 2, \dots, P_y$, with $P_y = (|\mathbb{G}_y| + 1)/2$. Accordingly, the coarray signals of the virtual subarray $\tilde{\mathbb{G}}_{(p_x, p_y)} = \mathbb{G}_x^{(p_x)} \cup \mathbb{G}_y^{(p_y)}$ can be partitioned from $\bar{\mathbf{V}}_{\mathbb{G}}$ as $\mathbf{U}_{\tilde{\mathbb{G}}_{(p_x, p_y)}} \in \mathbb{C}^{|\mathbb{G}_x^{(p_x)}| \times |\mathbb{G}_y^{(p_y)}|}$, defined as

$$\mathbf{U}_{\tilde{\mathbb{G}}_{(p_x, p_y)}} = \sum_{k=1}^K \sigma_k^4 \mathbf{g}_x^{(p_x)}(k) \circ \mathbf{g}_y^{(p_y)}(k), \quad (6)$$

where $\mathbf{g}_x^{(p_x)}(k) = [e^{-j\pi(2-p_x)\mu_1(k)}, e^{-j\pi(3-p_x)\mu_1(k)}, \dots, e^{-j\pi(q_{\mathbb{G}_x^{(1)}}+1-p_x)\mu_1(k)}]^T$ and $\mathbf{g}_y^{(p_y)}(k) = [e^{-j\pi(2-p_y)\mu_2(k)}, e^{-j\pi(3-p_y)\mu_2(k)}, \dots, e^{-j\pi(q_{\mathbb{G}_y^{(1)}}+1-p_y)\mu_2(k)}]^T$ serve as the steering vectors of $\mathbb{G}_x^{(p_x)}$ and $\mathbb{G}_y^{(p_y)}$, respectively.

Since the P_y virtual subarrays $\tilde{\mathbb{G}}_{(p_x, \cdot)}$ with a fixed index p_x share the same angular information along the x -axis while presenting a one-step shifting along the y -axis, concatenating their coarray signals along an additional shifting dimension contributes to a three-dimensional coarray tensor $\mathbf{U}_{(p_x)} \in \mathbb{C}^{|\mathbb{G}_x^{(p_x)}| \times |\mathbb{G}_y^{(1)}| \times P_y}$ as

$$\begin{aligned} \mathbf{U}_{(p_x)} &= \left[\mathbf{U}_{\tilde{\mathbb{G}}_{(p_x, 1)}}, \mathbf{U}_{\tilde{\mathbb{G}}_{(p_x, 2)}}, \dots, \mathbf{U}_{\tilde{\mathbb{G}}_{(p_x, P_y)}} \right]_{\sqcup_3} \\ &= \sum_{k=1}^K \sigma_k^4 \mathbf{g}_x^{(p_x)}(k) \circ \mathbf{g}_y^{(1)}(k) \circ \mathbf{q}_y(k) \\ &= \left[[\sigma_1^4, \sigma_2^4, \dots, \sigma_K^4]^T; \mathbf{G}_x^{(p_x)}, \mathbf{G}_y^{(1)}, \mathbf{Q}_y \right], \end{aligned} \quad (7)$$

where $\mathbf{g}_y^{(1)}(k)$ denotes the steering vector of the initial shifting window $\mathbb{G}_y^{(1)}$, and $\mathbf{q}_y(k) = [1, e^{j\pi\mu_2(k)}, \dots, e^{j\pi(P_y-1)\mu_2(k)}]^T$ denotes the shifting factor along the y -axis. Here, $\mathbf{G}_x^{(p_x)} = [\mathbf{g}_x^{(p_x)}(1), \mathbf{g}_x^{(p_x)}(2), \dots, \mathbf{g}_x^{(p_x)}(K)] \in \mathbb{C}^{|\mathbb{G}_x^{(p_x)}| \times K}$, $\mathbf{G}_y^{(1)} = [\mathbf{g}_y^{(1)}(1), \mathbf{g}_y^{(1)}(2), \dots, \mathbf{g}_y^{(1)}(K)] \in \mathbb{C}^{|\mathbb{G}_y^{(1)}| \times K}$, and $\mathbf{Q}_y = [\mathbf{q}_y(1), \mathbf{q}_y(2), \dots, \mathbf{q}_y(K)] \in \mathbb{C}^{P_y \times K}$ are the factor matrices of $\mathbf{U}_{(p_x)}$, $[\cdot]_{\sqcup_a}$ denotes the tensor concatenation operation along the a -th dimension, and $\llbracket \cdot \rrbracket$ denotes the canonical polyadic modeling of a tensor.

Since the angular information of the initial shifting window $\mathbb{G}_y^{(1)}$ and the shifting information along the y -axis jointly characterize the spatial information of the virtual subarrays $\tilde{\mathbb{G}}_{(p_x, \cdot)}$, all the P_x coarray tensors $\mathbf{U}_{(p_x)}$ present a strong relevance by coupling the common factor matrices $\mathbf{G}_y^{(1)}$ and \mathbf{Q}_y . Note that, the shifting coarray signals of the P_x virtual subarrays $\tilde{\mathbb{G}}_{(\cdot, p_y)}$ with a fixed index p_y can also be concatenated for generating coarray tensors with coupled angular information of the initial shifting window $\mathbb{G}_x^{(1)}$ and the corresponding shifting information along the x -axis.

C. Coupled Coarray Tensor CPD for DOA Estimation

To make full use of the spatial relevance among the formulated coarray tensors $\mathbf{U}_{(p_x)}$, the coupled coarray tensor CPD is proposed to jointly decompose them to estimate their respective factor matrices $\hat{\mathbf{G}}_x^{(p_x)}$, $p_x = 1, 2, \dots, P_x$, and the pair of coupled ones $\{\hat{\mathbf{G}}_y^{(1)}, \hat{\mathbf{Q}}_y\}$. Specifically, the summation of the canonical polyadic approximation error for all coarray tensors coupled in both angular and shifting dimensions is minimized by the following tensor-based least squares problem

$$\left\{ \hat{\mathbf{G}}_x^{(p_x)}, \hat{\mathbf{G}}_y^{(1)}, \hat{\mathbf{Q}}_y \right\} = \underset{\hat{\mathbf{G}}_x^{(p_x)}, \hat{\mathbf{G}}_y^{(1)}, \hat{\mathbf{Q}}_y}{\operatorname{argmin}} \sum_{p_x} \left\| \mathbf{U}_{(p_x)} - \llbracket \hat{\mathbf{G}}_x^{(p_x)}, \hat{\mathbf{G}}_y^{(1)}, \hat{\mathbf{Q}}_y \rrbracket \right\|_F^2, \quad (8)$$

where $\|\cdot\|_F$ denotes the Frobenius norm.

The coupled coarray tensor CPD optimization problem (8) can be solved by the alternative least squares (ALS) technique to yield $\{\hat{\mathbf{G}}_x^{(p_x)}, \hat{\mathbf{G}}_y^{(1)}, \hat{\mathbf{Q}}_y\}$ consisting of the estimated factors $\{\hat{\mathbf{g}}_x^{(p_x)}(k), \hat{\mathbf{g}}_y^{(1)}(k), \hat{\mathbf{q}}_y(k)\}$, $k = 1, 2, \dots, K$. According to the definition of $\{\mathbf{g}_x^{(p_x)}(k), \mathbf{g}_y^{(1)}(k), \mathbf{q}_y(k)\}$ established in Section III-B, their constituting directional parameters $(\hat{\mu}_1(k), \hat{\mu}_2(k))$ can be retrieved as

$$\begin{aligned} \hat{\mu}_1(k) &= \left(\sum_{p_x} \mathbf{v}_{(p_x)}^\dagger \angle \left(\hat{\mathbf{g}}_x^{(p_x)}(k) \right) / \pi \right) / P_x, \\ \hat{\mu}_2(k) &= \left(\mathbf{w}_{(1)}^\dagger \angle \left(\hat{\mathbf{g}}_y^{(1)}(k) \right) / \pi + \mathbf{z}^\dagger \angle \left(\hat{\mathbf{q}}_y(k) \right) / \pi \right) / 2, \end{aligned} \quad (9)$$

where $\mathbf{v}_{(p_x)} = [2 - p_x, 3 - p_x, \dots, q_{\mathbb{G}_x^{(1)}} + 1 - p_x]^T$ and $\mathbf{w}_{(1)} = [1, 2, \dots, q_{\mathbb{G}_y^{(1)}}]^T$ respectively represent the indices of virtual sensors in $\mathbb{G}_x^{(p_x)}$ and $\mathbb{G}_y^{(1)}$, and $\mathbf{z} = [0, 1, \dots, P_y - 1]^T$ represents the shifting steps along the y -axis. Here, $\angle(\cdot)$ denotes the phase of a complex number, and $(\cdot)^\dagger$ denotes the pseudoinverse operator. According to the relationship between the directional parameters $(\mu_1(k), \mu_2(k))$ and (θ_k, ϕ_k) defined in Section II, the closed-form azimuth and elevation angle of

the k -th source can then be estimated as

$$\hat{\theta}_k = \arctan(\hat{\mu}_2(k)/\hat{\mu}_1(k)), \hat{\phi}_k = \sqrt{\hat{\mu}_1^2(k) + \hat{\mu}_2^2(k)}. \quad (10)$$

IV. ANALYSIS ON THE ACHIEVABLE DOFs OF COUPLED COARRAY TENSOR CPD

Based on the uniqueness condition of the coupled CPD [34], the proposed coupled coarray tensor CPD is sufficiently unique if the following properties hold.

- (i) $\kappa(\mathbf{Q}_y) \geq 1$;
- (ii) $\min(|\mathbb{G}_x^{(p_x)}|, |\mathbb{G}_y^{(1)}|) \geq K - r(\mathbf{Q}_y) + 2$;
- (iii) $\begin{bmatrix} \mathbf{B}_m(\mathbf{G}_x^{(1)}) \odot \mathbf{B}_m(\mathbf{G}_y^{(1)}) \\ \vdots \\ \mathbf{B}_m(\mathbf{G}_x^{(P_x)}) \odot \mathbf{B}_m(\mathbf{G}_y^{(1)}) \end{bmatrix} \in \mathbb{C}^{\left(\begin{smallmatrix} P_x C_m^{|\mathbb{G}_x^{(p_x)}|} C_m^{|\mathbb{G}_y^{(1)}|} \\ \times C_m^K \end{smallmatrix} \right) \times C_m^K}$ has a full column rank, where $m = K - r(\mathbf{Q}_y) + 2$, and $\mathbf{B}_m(\mathbf{G}_x^{(1)}) \in \mathbb{C}^{C_m^{|\mathbb{G}_x^{(1)}|} \times C_m^K}$ is the m -th compound matrix of $\mathbf{G}_x^{(1)}$;
- (iv) There exists a subset $\mathbb{T} \subseteq \{1, 2, \dots, K\}$ to guarantee that $[\mathbf{Q}_y]_{\mathbb{T}} \in \mathbb{C}^{P_y \times |\mathbb{T}|}$, $[\mathbf{G}_x^{(p_x)}]_{\bar{\mathbb{T}}} \in \mathbb{C}^{|\mathbb{G}_x^{(p_x)}| \times (K - |\mathbb{T}|)}$ and $[\mathbf{G}_y^{(1)}]_{\bar{\mathbb{T}}} \in \mathbb{C}^{|\mathbb{G}_y^{(1)}| \times (K - |\mathbb{T}|)}$ have a full column rank, where $[\mathbf{Q}_y]_{\mathbb{T}}$ stacks the columns of \mathbf{Q}_y indexed by \mathbb{T} with $|\mathbb{T}| \leq r(\mathbf{Q}_y)$, and $\bar{\mathbb{T}}$ is the complement set of \mathbb{T} .

Here, $\kappa(\cdot)$ denotes the Kruskal rank, $r(\cdot)$ denotes the matrix rank, $C_j^l = \frac{j!}{l!(j-l)!}$ denotes the binomial coefficient, and \odot denotes the Khatri-Rao product.

For the formulated coupled coarray tensors $\mathbf{U}_{(p_x)}$, since we have $\kappa(\mathbf{Q}_y) = \min(P_y, K) = P_y$, the property $\kappa(\mathbf{Q}_y) \geq 1$ is satisfied. Then, when deploying a CLsA with $|\mathbb{L}_1| \leq |\mathbb{L}_2|$, we have $\min(|\mathbb{G}_x^{(p_x)}|, |\mathbb{G}_y^{(1)}|) = |\mathbb{G}_x^{(p_x)}|$, such that the Property (ii) can be satisfied as long as

$$|\mathbb{G}_x^{(p_x)}| + P_y - 2 \geq K. \quad (11)$$

Based on such an upper bound for K in (11) and the resulting upper bound $m \leq |\mathbb{G}_x^{(p_x)}|$, Property (iii) can be guaranteed thanks to its relaxed constraint. Moreover, the subset \mathbb{T} ensures that the factor matrix of the coupled coarray tensors $[\mathbf{Q}_y]_{\mathbb{T}}$ has a full column rank due to $|\mathbb{T}| \leq P_y$. Meanwhile, considering $K - |\mathbb{T}| \leq \min(|\mathbb{G}_x^{(p_x)}|, |\mathbb{G}_y^{(1)}|)$, $[\mathbf{G}_x^{(p_x)}]_{\bar{\mathbb{T}}}$ and $[\mathbf{G}_y^{(1)}]_{\bar{\mathbb{T}}}$ also have a full column rank since all their columns are non-collinear. Therefore, the achievable number of DOFs for the proposed coupled coarray tensor CPD-based DOA estimation method is $|\mathbb{G}_x^{(p_x)}| + P_y - 2$, which exceeds the number of physical sensors in the designed CLsA. This implies that the proposed method maintains an increased number of DOFs.

V. SIMULATION RESULTS

Consider the CLsA with $M_{\mathbb{L}_1} = M_{\mathbb{L}_2} = 2$ and $N_{\mathbb{L}_1} = N_{\mathbb{L}_2} = 3$, where the total number of sensors is 12. As such, the derived virtual UCA \mathbb{G} contains $|\mathbb{G}_x| = 15$ and $|\mathbb{G}_y| = 15$ virtual sensors in the x, y -axes, respectively. Thus, we have $|\mathbb{G}_x^{(p_x)}| = 8$ and $P_y = 8$, resulting the achievable number of DOFs to be $|\mathbb{G}_x^{(p_x)}| + P_y - 2 = 14$. The ordinary CPD and the coupled coarray tensor CPD are both implemented with the tensorlab 3.0 [35].

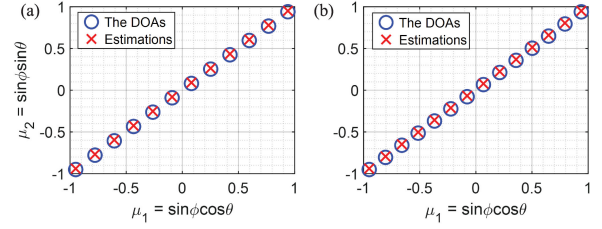


Fig. 3. Underdetermined DOA estimation performance of the proposed method. (a) $K = 12$ sources; (b) $K = 14$ sources.

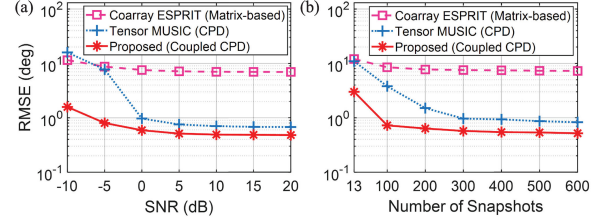


Fig. 4. Estimation accuracy comparison. (a) RMSE versus SNR, $T = 300$; (b) RMSE versus snapshots, SNR = 0 dB.

The underdetermined DOA estimation performance of the proposed method is presented in Fig. 3 with noise-free snapshots, where the cases of $K = 12$ and $K = 14$ sources with μ_1 and μ_2 both uniformly distributed in $[-0.94, 0.94]$ are considered. It is clear that the proposed method is capable of locating all sources in the underdetermined circumstances, which validates the increased number of DOFs contributed by the designed coupled coarray tensor CPD.

Then, the estimation accuracy of the proposed method is compared to the coarray ESPRIT method with a matrix-based processing technique [36] and the coarray-based tensor MUSIC method using the ordinary CPD approach [18]. Two sources are assumed to impinge on the CLsA from $(\theta_1, \phi_1) = (20.5^\circ, 30.5^\circ)$ and $(\theta_2, \phi_2) = (45.6^\circ, 40.6^\circ)$, and 1,000 Monte-Carlo trials are performed to calculate the root-mean-square error (RMSE) for each scenario. It is demonstrated in Fig. 4 that the proposed coupled coarray tensor CPD-based DOA estimation method exhibits a significant improvement in estimation accuracy than the coarray ESPRIT method due to the tensor-based modeling for coarray statistics. In addition, the proposed method also outperforms the coarray-based tensor MUSIC method especially under the conditions of low SNR and limited snapshots. It is because that the proposed coupled coarray tensor CPD approach fully exploits the spatial relevance among the formulated coarray tensors, which is ignored by directly applying ordinary CPD on a spatially smoothed coarray tensor.

VI. CONCLUSION

A coupled coarray tensor CPD-based DOA estimation method was proposed for a specially designed coprime L-shaped array. The shifting coarray concatenation approach is developed to formulate multiple coupled coarray tensors for joint decomposition. Due to the utilization of spatial relevance among these coarray tensors, the DOA estimation accuracy is effectively improved with an increased number of DOFs.

REFERENCES

- [1] P. P. Vaidyanathan and P. Pal, "Sparse sensing with co-prime samplers and arrays," *IEEE Trans. Signal Process.*, vol. 59, no. 2, pp. 573–586, Feb. 2011.
- [2] C. Zhou, Y. Gu, X. Fan, Z. Shi, G. Mao, and Y. D. Zhang, "Direction-of-arrival estimation for coprime array via virtual array interpolation," *IEEE Trans. Signal Process.*, vol. 66, no. 22, pp. 5956–5971, Nov. 2018.
- [3] X. Wu, W.-P. Zhu, and J. Yan, "A Toeplitz covariance matrix reconstruction approach for direction-of-arrival estimation," *IEEE Trans. Veh. Technol.*, vol. 66, no. 9, pp. 8223–8237, Sep. 2017.
- [4] C. Zhou, Y. Gu, S. He, and Z. Shi, "A robust and efficient algorithm for coprime array adaptive beamforming," *IEEE Trans. Veh. Technol.*, vol. 67, no. 2, pp. 1099–1122, Feb. 2018.
- [5] C. Zhou, Y. Gu, Y. D. Zhang, Z. Shi, T. Jin, and X. Wu, "Compressive sensing-based coprime array direction-of-arrival estimation," *IET Commun.*, vol. 11, no. 11, pp. 1719–1724, Aug. 2017.
- [6] J. Li, Y. He, X. Zhang, and Q. Wu, "Simultaneous localization of multiple unknown emitters based on UAV monitoring big data," *IEEE Trans. Ind. Inform.*, vol. 17, no. 9, pp. 6303–6313, Sep. 2021.
- [7] C. Zhou, Z. Shi, Y. Gu, and X. Shen, "DECOM: DOA estimation with combined MUSIC for coprime array," in *Proc. Int. Conf. Wireless Commun. Signal Process.*, Hangzhou, China, Oct. 2013, pp. 1–5.
- [8] Y. Gu and A. Leshem, "Robust adaptive beamforming based on interference covariance matrix reconstruction and steering vector estimation," *IEEE Trans. Signal Process.*, vol. 60, no. 7, pp. 3881–3885, Jul. 2012.
- [9] K. Han and A. Nehorai, "Nested vector-sensor array processing via tensor modeling," *IEEE Trans. Signal Process.*, vol. 62, no. 10, pp. 2542–2553, May 2014.
- [10] S. Na, K. V. Mishra, Y. Liu, Y. C. Eldar, and X. Wang, "TenDSuR: Tensor-based 4D sub-Nyquist radar," *IEEE Signal Process. Lett.*, vol. 26, no. 2, pp. 237–241, Feb. 2019.
- [11] H. Zheng, C. Zhou, Y. Gu, and Z. Shi, "Two-dimensional DOA estimation for coprime planar array: A coarray tensor-based solution," in *Proc. IEEE Int. Conf. Acoust., Speech, Signal Process.*, Barcelona, Spain, May 2020, pp. 4562–4566.
- [12] H. Zheng, C. Zhou, Y. Wang, and Z. Shi, "2-D DOA estimation for coprime cubic array: A cross-correlation tensor perspective," in *Proc. Int. Symp. Antennas Propag.*, Osaka, Japan, Jan. 2021, pp. 447–448.
- [13] C. Zhou, Y. Gu, Z. Shi, and Y. D. Zhang, "Off-grid direction-of-arrival estimation using coprime array interpolation," *IEEE Signal Process. Lett.*, vol. 25, no. 11, pp. 1710–1714, Nov. 2018.
- [14] X. Wu and W.-P. Zhu, "Single far-field or near-field source localization with sparse or uniform cross array," *IEEE Trans. Veh. Technol.*, vol. 69, no. 8, pp. 9135–9139, Aug. 2020.
- [15] Z. Shi, C. Zhou, Y. Gu, N. A. Goodman, and F. Qu, "Source estimation using coprime array: A sparse reconstruction perspective," *IEEE Sensors J.*, vol. 17, no. 3, pp. 755–765, Feb. 2017.
- [16] J. Li, P. Ma, X. Zhang, and G. Zhao, "Improved DFT algorithm for 2D DOA estimation based on 1D nested array motion," *IEEE Commun. Lett.*, vol. 24, no. 9, pp. 1953–1956, Sep. 2020.
- [17] X. Wu, "Localization of far-field and near-field signals with mixed sparse approach: A generalized symmetric arrays perspective," *Signal Process.*, vol. 175, Oct. 2020, Art. no. 107665.
- [18] C.-L. Liu and P. P. Vaidyanathan, "Tensor MUSIC in multidimensional sparse arrays," in *Proc. Asilomar Conf. Signals, Syst. Comput.*, Pacific Grove, CA, USA, Nov. 2015, pp. 1783–1787.
- [19] J. Shi, D. Wu, and Z. Li, "Tensor-based angle estimation with coprime MIMO radar," in *Proc. IEEE Sensor Array Multichannel Signal Process. Workshop*, Hangzhou, China, Jun. 2020, pp. 1–4.
- [20] J. Shi, F. Wen, and T. Liu, "Nested MIMO radar: Coarrays, tensor modeling, and angle estimation," *IEEE Trans. Aerosp. Electron. Syst.*, vol. 57, no. 1, pp. 573–585, Feb. 2021.
- [21] M. Sørensen and L. De Lathauwer, "Coupled tensor decompositions for applications in array signal processing," in *Proc. IEEE Int. Workshop Comput. Adv. Multi-Sensor Adaptive Process.*, Saint Martin, France, Dec. 2013, pp. 228–231.
- [22] M. Sørensen and L. De Lathauwer, "Multidimensional harmonic retrieval via coupled canonical polyadic decompositions-Part I: Model and identifiability," *IEEE Trans. Signal Process.*, vol. 65, no. 2, pp. 517–527, Jan. 2017.
- [23] M. Sørensen and L. De Lathauwer, "Multidimensional harmonic retrieval via coupled canonical polyadic decompositions-Part II: Algorithm and multirate sampling," *IEEE Trans. Signal Process.*, vol. 65, no. 2, pp. 528–539, Jan. 2017.
- [24] X. Gong, Q. Lin, F. Gong, and L. De Lathauwer, "Double coupled canonical polyadic decomposition for joint blind source separation," *IEEE Trans. Signal Process.*, vol. 66, no. 13, pp. 3475–3490, Jul. 2018.
- [25] B. Sokal, A. L. F. de Almeida, and M. Haardt, "Semi-blind receivers for MIMO multi-relaying systems via rank-one tensor approximations," *Signal Process.*, vol. 166, Jan. 2020, Art. no. 107254.
- [26] Y. Bu *et al.*, "Hyperspectral and multispectral image fusion via graph Laplacian-guided coupled tensor decomposition," *IEEE Trans. Geosci. Remote Sens.*, vol. 59, no. 1, pp. 648–662, Jan. 2021.
- [27] R. A. Borsoi, C. Prévost, K. Usevich, D. Brie, J. C. M. Bermudez, and C. Richard, "Coupled tensor decomposition for hyperspectral and multispectral image fusion with inter-image variability," *IEEE J. Sel. Topics Signal Process.*, vol. 15, no. 3, pp. 702–717, Apr. 2021.
- [28] B. Hunyadi, P. Dupont, W. Van Paesschen, and S. Van Huffel, "Tensor decompositions and data fusion in epileptic electroencephalography and functional magnetic resonance imaging data," *WIREs Data Mining Knowl. Discov.*, vol. 7, no. 1, Jan. 2017, Art. no. e1197.
- [29] K. Naskovska, S. Lau, A. A. Korobkov, J. Hauelsen, and M. Haardt, "Coupled CP decomposition of simultaneous MEG-EEG signals for differentiating oscillators during photic driving," *Front. Neurosci.*, vol. 14, Apr. 2020, Art. no. 261.
- [30] M. Sørensen and L. De Lathauwer, "Multiple invariance ESPRIT for nonuniform linear arrays: A coupled canonical polyadic decomposition approach," *IEEE Trans. Signal Process.*, vol. 64, no. 14, pp. 3693–3704, Jul. 2016.
- [31] M. Sørensen, I. Domanov, and L. De Lathauwer, "Coupled canonical polyadic decompositions and multiple shift invariance in array processing," *IEEE Trans. Signal Process.*, vol. 66, no. 14, pp. 3665–3680, Jul. 2018.
- [32] X. Wu, W.-P. Zhu, and J. Yan, "Gridless two-dimensional DOA estimation with L-shaped array based on the cross-covariance matrix," in *Proc. IEEE Int. Conf. Acoust., Speech, Signal Process.*, Calgary, Canada, Apr. 2018, pp. 3256–3260.
- [33] Y. Dong, C. Dong, W. Liu, H. Chen, and G. Zhao, "2-D DOA estimation for L-shaped array with array aperture and snapshots extension techniques," *IEEE Signal Process. Lett.*, vol. 24, no. 4, pp. 495–499, Apr. 2017.
- [34] M. Sørensen and L. De Lathauwer, "Coupled canonical polyadic decompositions and (coupled) decompositions in multilinear rank- $(L_{r,n}, L_{r,n}, 1)$ terms-part I: Uniqueness," *SIAM J. Matrix Anal. Appl.*, vol. 36, no. 2, pp. 496–522, May 2015.
- [35] N. Vervliet, O. Debals, L. Sorber, M. Van Barel, and L. De Lathauwer, *Tensorlab 3.0*, Mar. 2016. [Online]. Available: URL: <http://www.tensorlab.net>
- [36] C. Zhou and J. Zhou, "Direction-of-arrival estimation with coarray ESPRIT for coprime array," *Sensors*, vol. 17, no. 8, Aug. 2017, Art. no. 1779.